Electronic Supplementary Material (ESI) for Physical Chemistry Chemical Physics

Supporting Information

"Ground state depletion microscopy for imaging interactions between gold nanowires and fluorophore-labelled ligands"

K. L. Blythe, K. M. Mayer, M.L. Weber, K.A. Willets

Table of contents:

Jablonski diagram for GSDIM

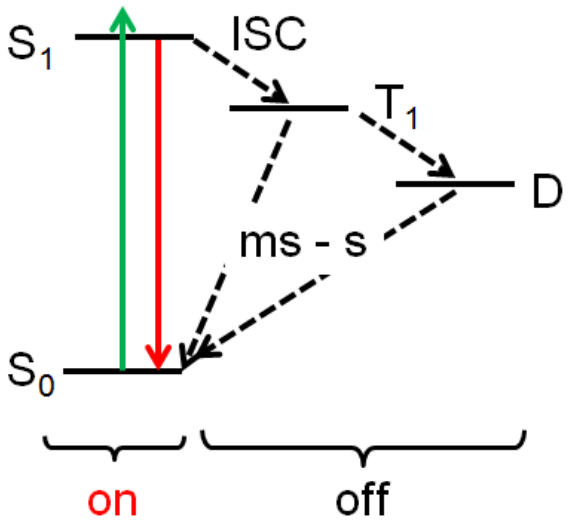

Figure S-1. Jablonski diagram showing how the ground state depletion process works. A fluorophore is excited from the electronic ground state (S_0) to the first electronic excited state (S_1) and emits a fluorescent photon with a probability given by the fluorescence quantum yield. This is the "on" state of the molecule. Eventually, the molecule will inter-system cross (ISC) into the triplet state (T_1) from where it can also enter metastable dark states (D). This represents the "off" state of the molecule. By controlling the excitation intensity, we can control the number of molecules that are shelved in the off state.

Image processing and point spread function fitting.

All image processing is performed MATLAB code developed in-house, following the procedure described here. As described the main text of this article, gold nanowires exhibit a strong luminescence background[1-4], which must be removed before fitting the point spread function of the emitting fluorophore. To identify emitting molecules above the luminescent background on the gold nanowire, we process our data as follows. First, we identify the nanowire of interest and rotate the image so it is vertically oriented (Figure S-2, A and B).

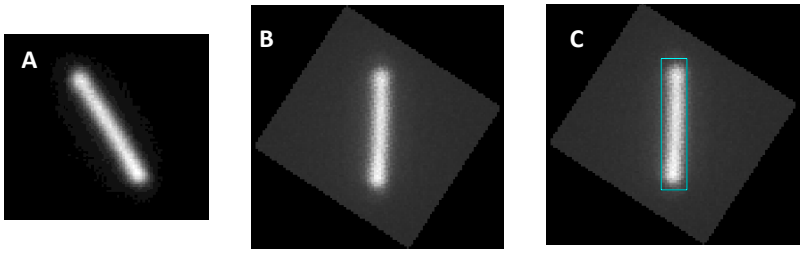

Figure S-2. (A) Original nanowire image. (B) Rotated nanowire image. (C) Selected region of interest of nanowire.

Next, we define the edges of the nanowire (cyan box, Figure S-2C) and slice the nanowire into subsections, with a width correlated to the diffraction limited spot size (*w* in Figure S-3A) and a step size of 0.5**w*. We calculate the intensity of each subsection as shown in Figure S-3B.

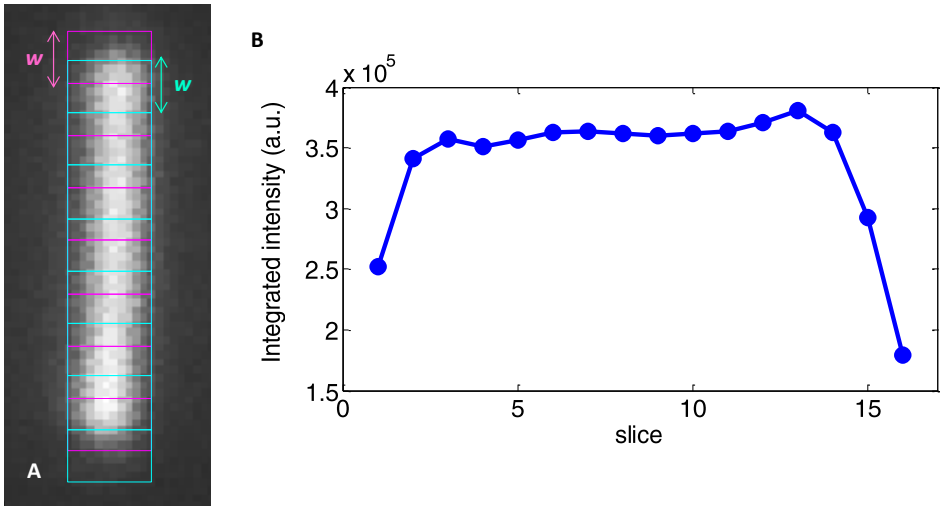

Figure S-3. (A) Defining the individual slices of the nanowire. Each slice has width *w* and each slice starts at a distance of 0.5**w* from the previous slice. Alternating slices are labeled in cyan and magenta for clarity. (B) Integrated intensity from each subsection of the nanowire along its length.

This process is repeated for every frame in our image stack to generate a series of intensity plots corresponding to each frame of the movie (Fig. S-3B, Fig S-4A). Next, we subtract the intensity plots of adjacent images as shown in Figure S-4B.

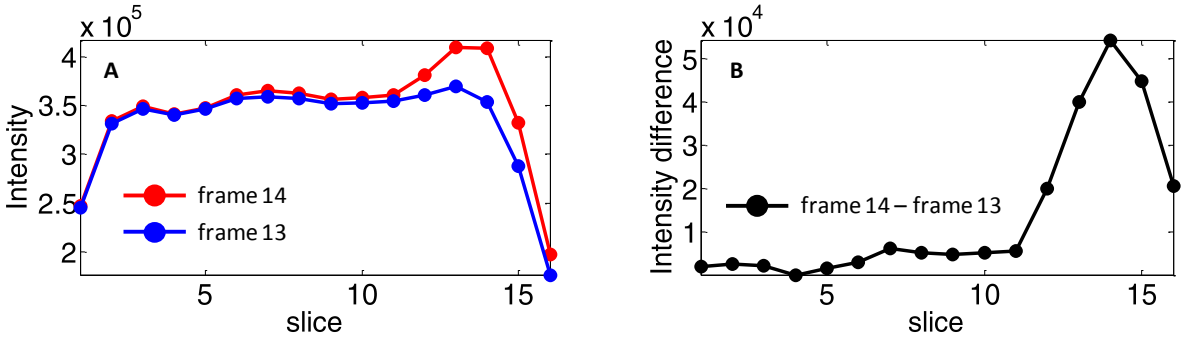

Figure S-4. (A) Integrated intensity for two adjacent frames in the image stack. (B) Intensity difference for the two plots shown in (A).

The large intensity spike seen around slice 14 indicates the presence of a molecule above the nanoparticle luminescence background. This process is repeated for all frames in the image stack. We then calculate three times the standard deviation of the intensity difference for each slice (Figure S-5, black dashed line) and identify frames where the intensity difference is higher than this threshold value (Figure S-5). These frames are then subjected to further processing.

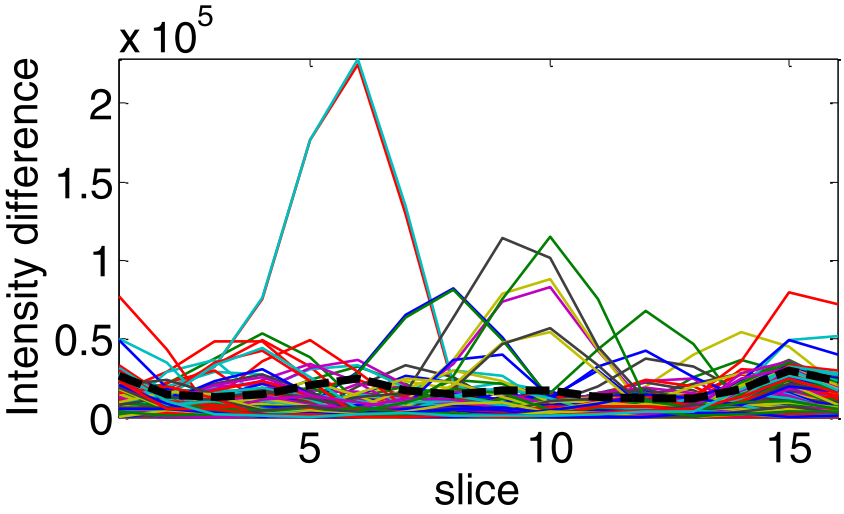

Figure S-5. Intensity difference calculations for 1873 adjacent frames in the original image stack. Three times the standard deviation of the difference for each slice is calculated and plotted as the dashed black line.

Next, we return to the original, unprocessed images, as shown in Figure S-6A. For each frame with a potential "on" event, we subtract the nanoparticle luminescence background in order to isolate the signal for the molecule. To do this, we calculate the average luminescence from up to four frames that immediately precede the frame of interest, but do not have signal above our previously determined threshold. This composite background (Figure S-6B) is then subtracted from our frame of interest (Figure S-6A) to produce an image in which only signal from the molecule is present (Figure S-6C).

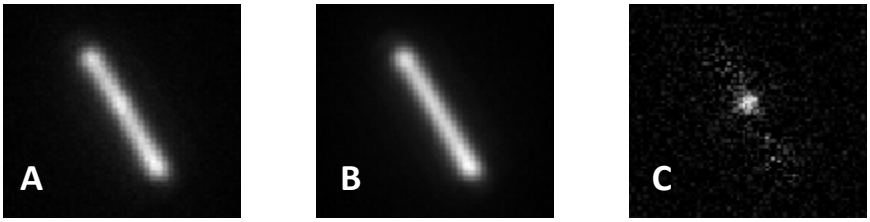

Figure S-6. (A) Raw image from the frame of interest. (B) Average background from up to four image frames below the threshold. (C) Subtracted image showing the location of the emitting molecule.

Next, we smooth the subtracted image (Figure S-6C is reproduced in Figure S-7A) with a Gaussian filter (Figure S-7B) and digitize the image (Figure S-7C). This allows us to remove any background noise and identify signal coming from actual molecules. We find the centroid (x_c, y_c) of the molecule in the digital image in Figure S-7C, and this is used as an initial guess for (x_0, y_0) in our least squares fit. The initial guess for the intensity is the intensity of the subtracted image (Figure S-7A) at (x_c, y_c) while the offset guess is set at zero, since the background has been pre-subtracted. The initial guesses for the widths of the Gaussian (s_x and s_y) are arbitrarily set at 3 pixels. Using these initial guesses, a nonlinear least squares fit of the original, raw data from Figure S-7A to equation 1 in the main text is performed; the resulting fit is shown in Figure S-7D.

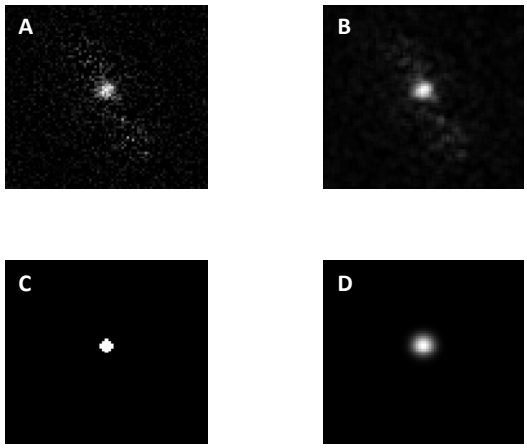

Figure S-7. (A) Subtracted image reproduced from Fig XXA. (B) Image from (A) smoothed with a Gaussian filter. (C) Digitized version of the image from (B) which removes any spurious noise. (D) 2-D Gaussian fit of the image from (A).

The code is designed to identify and fit multiple molecules that may be on in the same frame, as shown in Figure S-8. The same procedure is followed, except each molecule in the digital image is assigned a unique identifier, from which the initial guesses are derived. Each molecule is fit to a single Gaussian, as described above. Note that a weak emitter in this image is not counted due to low signal-to-noise.

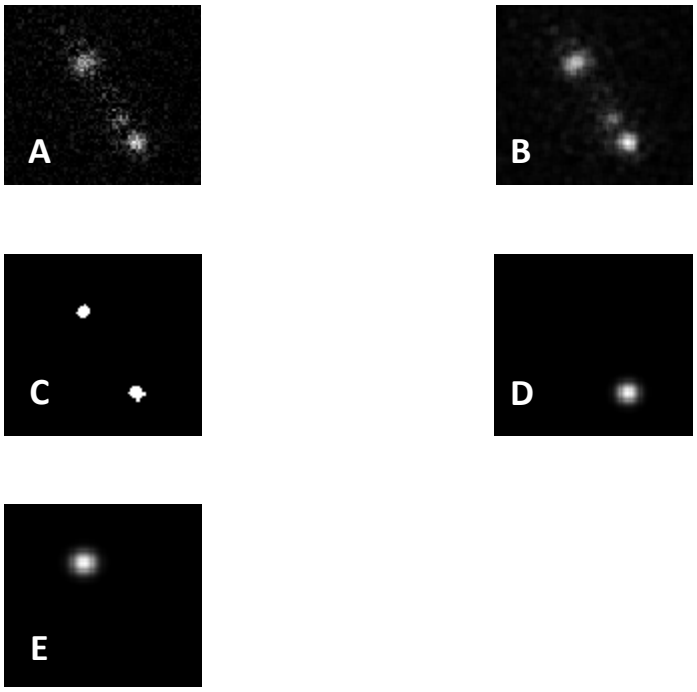

Figure S-8. (A) Subtracted image, (B) smoothed image after application of Gaussian filter, (C) digitized image showing two molecules to be fit. (D) Gaussian fit to the molecule in the lower right and (E) Gaussian fit to the molecule in the upper left.

Lastly, all fits are subjected to a final filtering step in which the following filters are applied:

- s_x and s_y must be within 80% of each other; otherwise, the fit is rejected.
- s_x and s_y must be greater than 1 pixel and less than 5 pixels; otherwise, the fit is rejected.
- In the case of multiple molecules (as in Figure S-8), centroids cannot be within 6 pixels of each other; otherwise, both fits are rejected.

All molecules that make it through this final screening step are then drift-corrected using our alignment markers.[5] The corrected (x_0, y_0) coordinates are then plotted as shown in Figure S-9.

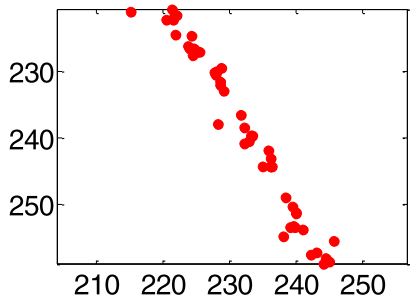

Figure S-9. Calculated centroid coordinates for all molecules fit for the nanorod discussed above.

Comparing labeled vs. unlabeled nanowires

Even in the absence of fluorophore labels, nanowires can still show dynamics in their fluorescence time traces (Figure S-10A). For the unlabeled nanowire, only 7 bursts of intensity could be localized for the 120 seconds of data acquisition, Figure S-10C. However, the labeled wire yielded 38 localized bursts for the same time frame, Figure S-10F. When we process the unlabeled nanowire using the same procedure described above, we find that most of the spurious intensity bursts do not make it through the first step of our fitting procedure (Figure S-11). Moreover, the nanowire bursts are only 5% above the background luminescence whereas most of the TAMRA bursts are >20% above the background.

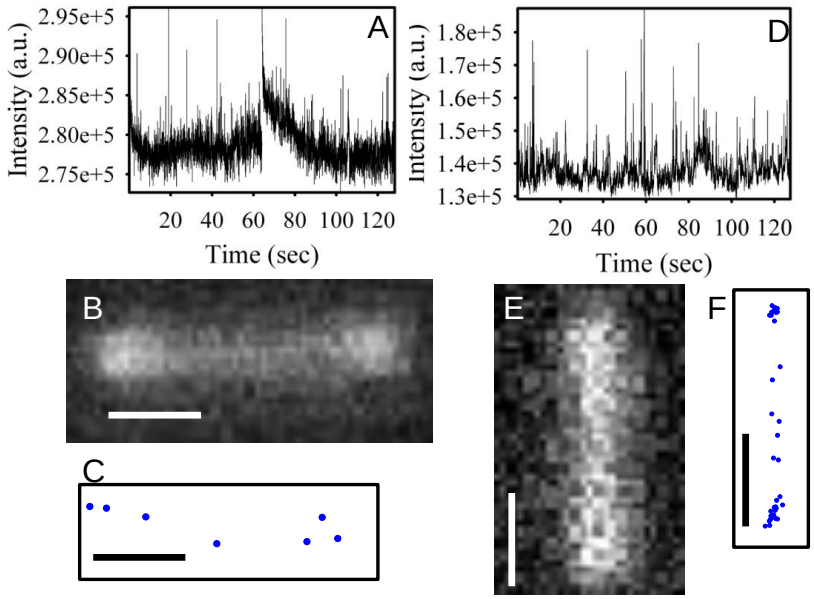

Figure S-10. (A) Integrated intensity time trace showing bursts associated with gold nanowire luminescence blinking. (B) Luminescence image of the unlabeled nanowire. (C) Scatter plot showing the values of (x_0, y_0) for the Gaussian fits to each luminescence burst. (D) Integrated intensity time trace showing fluorescence bursts associated with GSDIM. (E) Fluorescence image of the labeled nanowire. (F) Scatter plot showing the values of (x_0, y_0) for the Gaussian fits to each fluorescent burst. A-C have a common 500 nm scale bar. D-F have a common 500 nm scale bar.

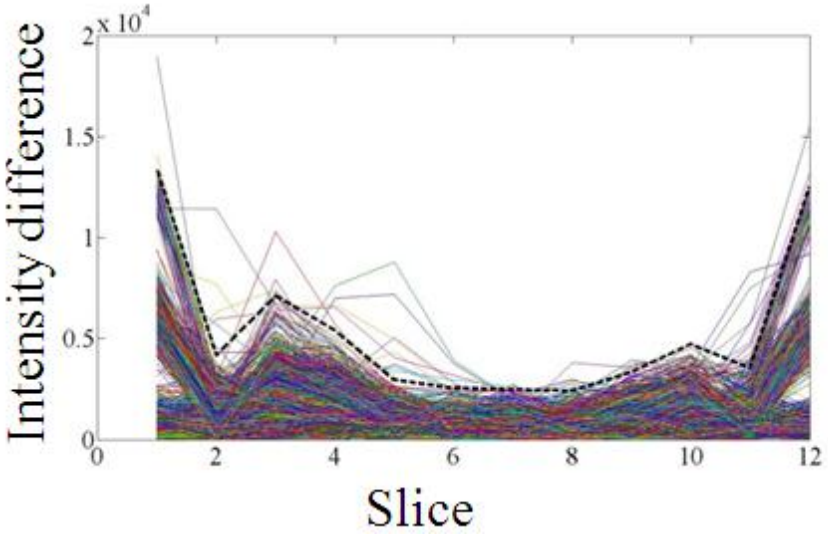

Figure S-11. Intensity difference calculations for 1874 adjacent frames in the first original image stack for a bare gold nanowire. Three times the standard deviation of the difference for each slice is calculated and plotted as the dashed black line.

Scatter plot and histograms of reconstructed wires discussed in the paper.

For completeness, we show the original scatter plots for all wires shown in the manuscript. In the scatter plots, each data point corresponds to the centroid position of a single fluorescent burst identified through the procedure described above. We also include both the relative frequency histograms and spatial intensity maps with different bin sizes (2, 10, and 20 nm) for comparison to the histograms with 40 nm bin size shown in the manuscript. The 2 nm bins are almost impossible to see relative to the large overall size of the histogram, which is dictated by the length of the nanowires. Trends observed in the 40 nm bin histograms from the manuscript are retained in the 10 and 20 nm binned histograms.

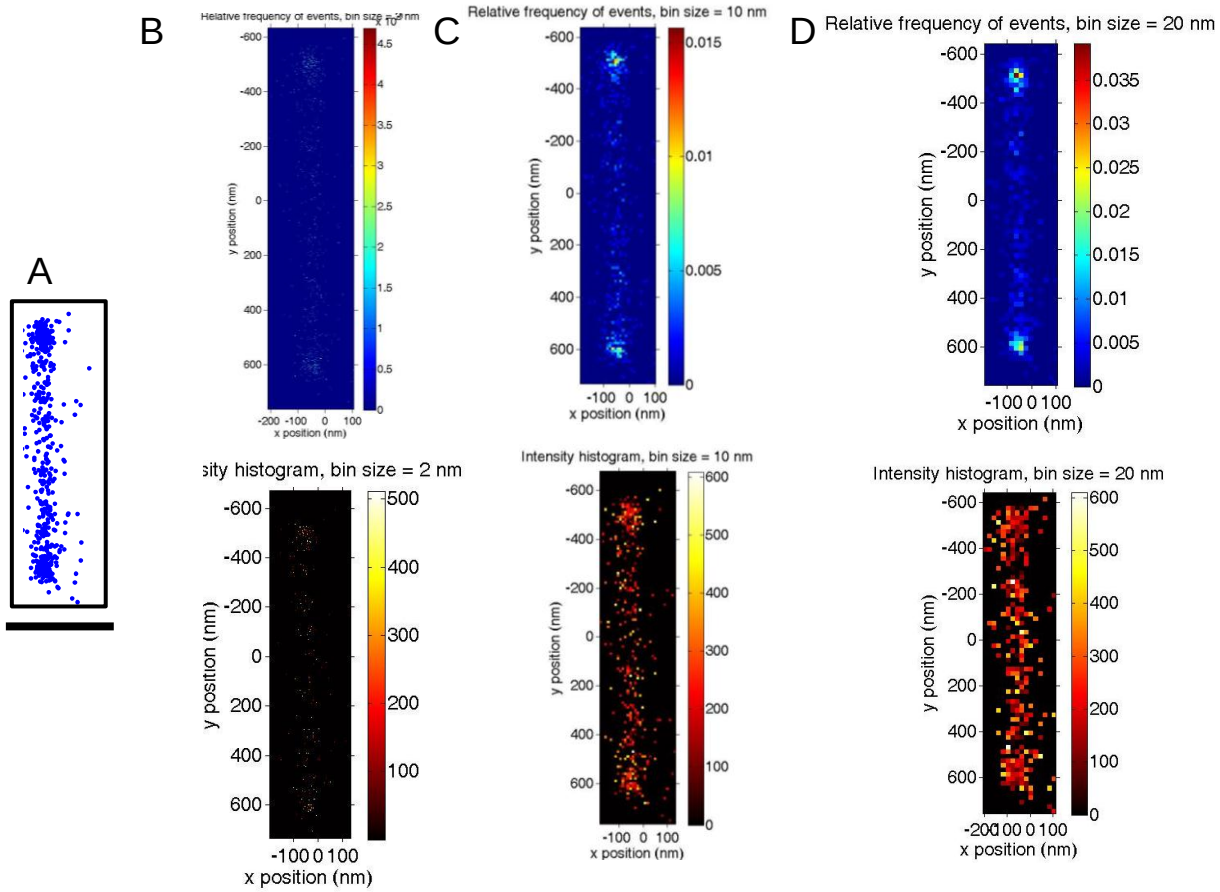

Figure S-12. Data associated with Figure 1 from the manuscript. (A) Scatter plot of centroid points. Scale bar is 500 nm. (B-D) (top) Relative frequency histograms and (bottom) spatial intensity maps with bin sizes of (B) 2 nm, (C) 10 nm and (D) 20 nm. Scale is as marked.

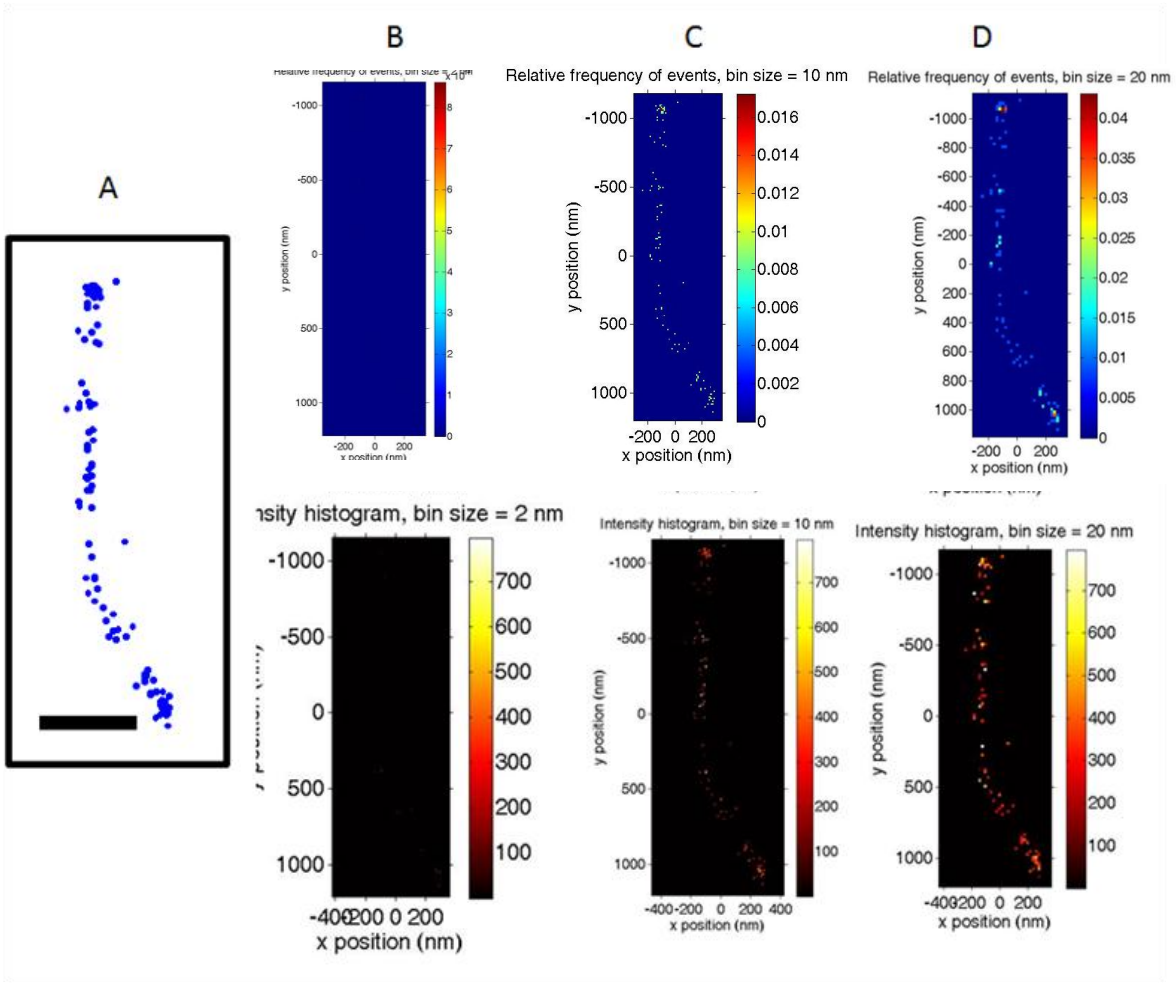

Figure S-13. Data associated with Figure 2A-D from the manuscript. (A) Scatter plot of centroid points. Scale bar is 500 nm. (B-D) (top) Relative frequency histograms and (bottom) spatial intensity maps with bin sizes of (B) 2 nm, (C) 10 nm and (D) 20 nm. Scale is as marked.

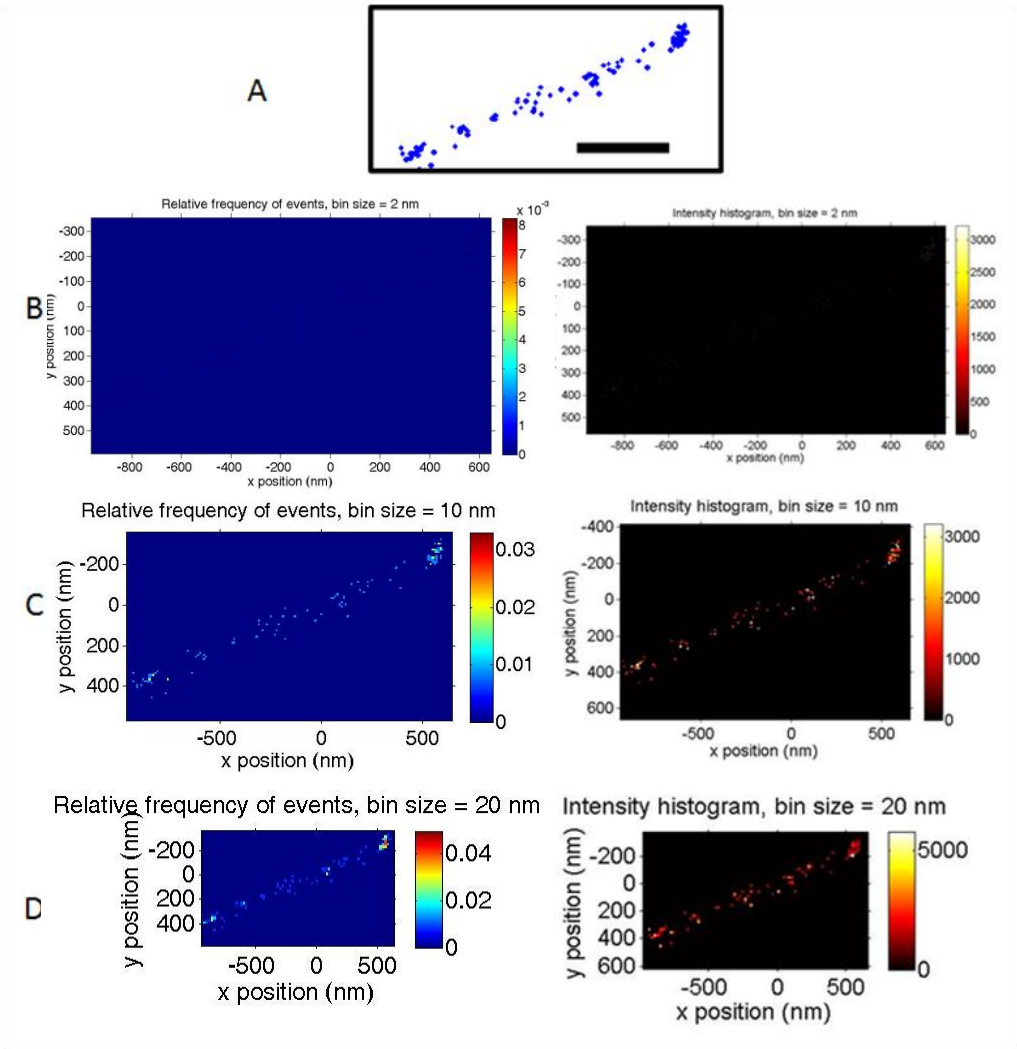

Figure S-14. Data associated with Figure 2E-H from the manuscript. (A) Scatter plot of centroid points. Scale bar is 500 nm. (B-D) (left) Relative frequency histograms and (right) spatial intensity maps with bin sizes of (B) 2 nm, (C) 10 nm and (D) 20 nm. Scale is as marked.

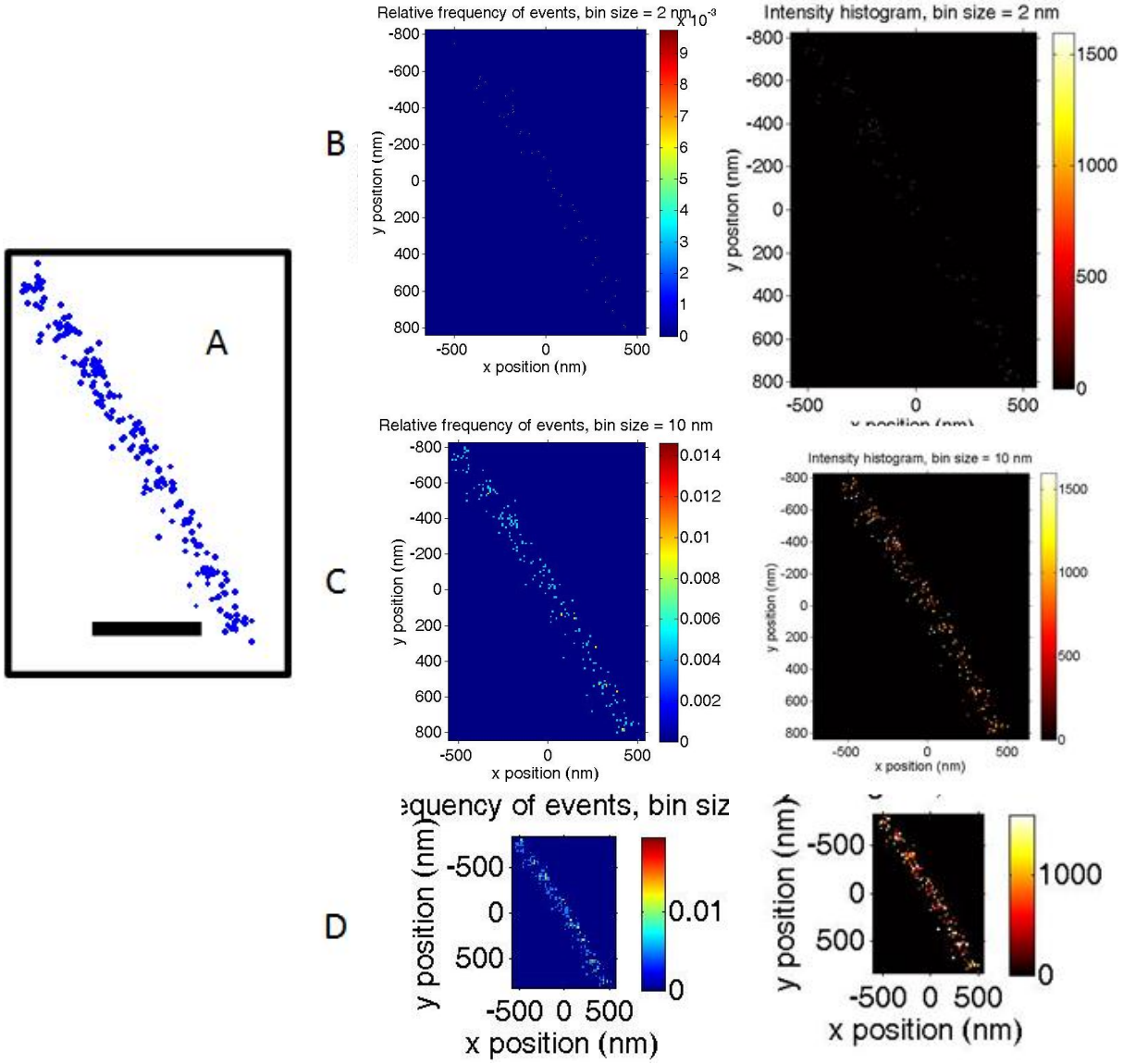

Figure S-15. Data associated with Figure 3 from the manuscript. (A) Scatter plot of centroid points. Scale bar is 500 nm. (B-D) (left) Relative frequency histograms and (right) spatial intensity maps with bin sizes of (B) 2 nm, (C) 10 nm and (D) 20 nm. Scale is as marked.

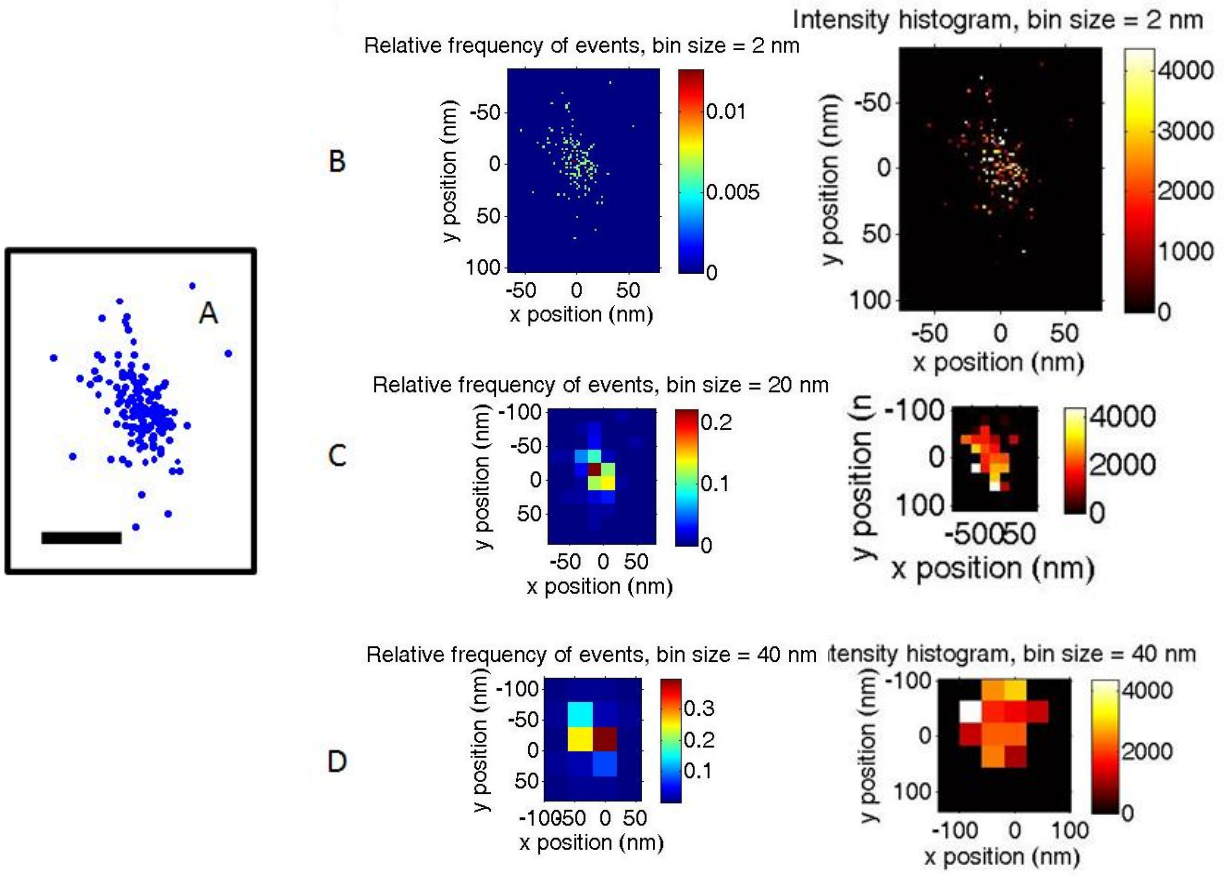

Figure S-16. Data associated with Figure 4 from the manuscript. (A) Scatter plot of centroid points. Scale bar is 50 nm. (B-D) (left) Relative frequency histograms and (right) spatial intensity maps with bin sizes of (B) 2 nm, (C) 20 nm and (D) 40 nm. Scale is as marked.

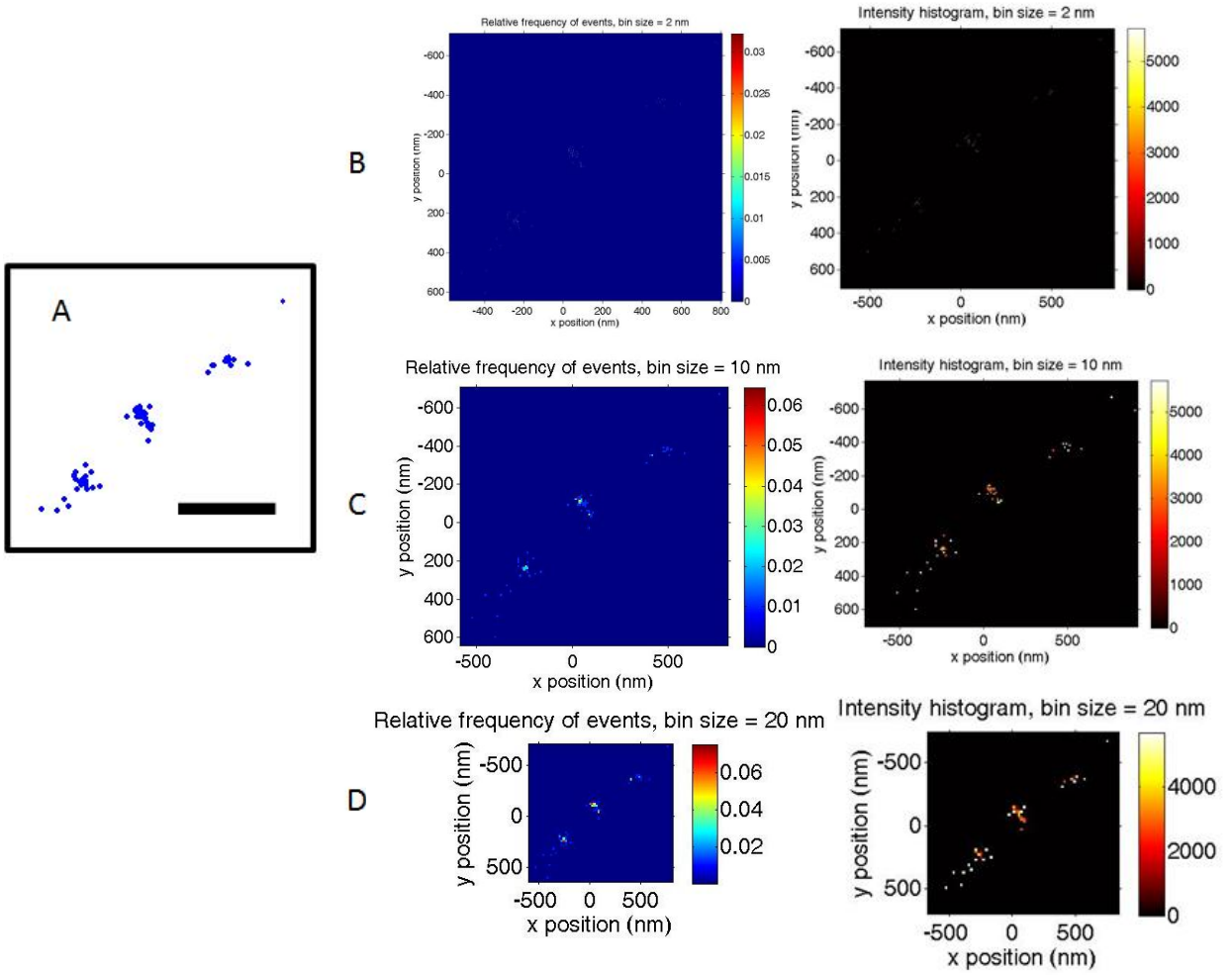

Figure S-17. Data associated with Figure 5 from the manuscript. (A) Scatter plot of centroid points. Scale bar is 500 nm. (B-D) (left) Relative frequency histograms and (right) spatial intensity maps with bin sizes of (B) 2 nm, (C) 10 nm and (D) 20 nm. Scale is as marked.

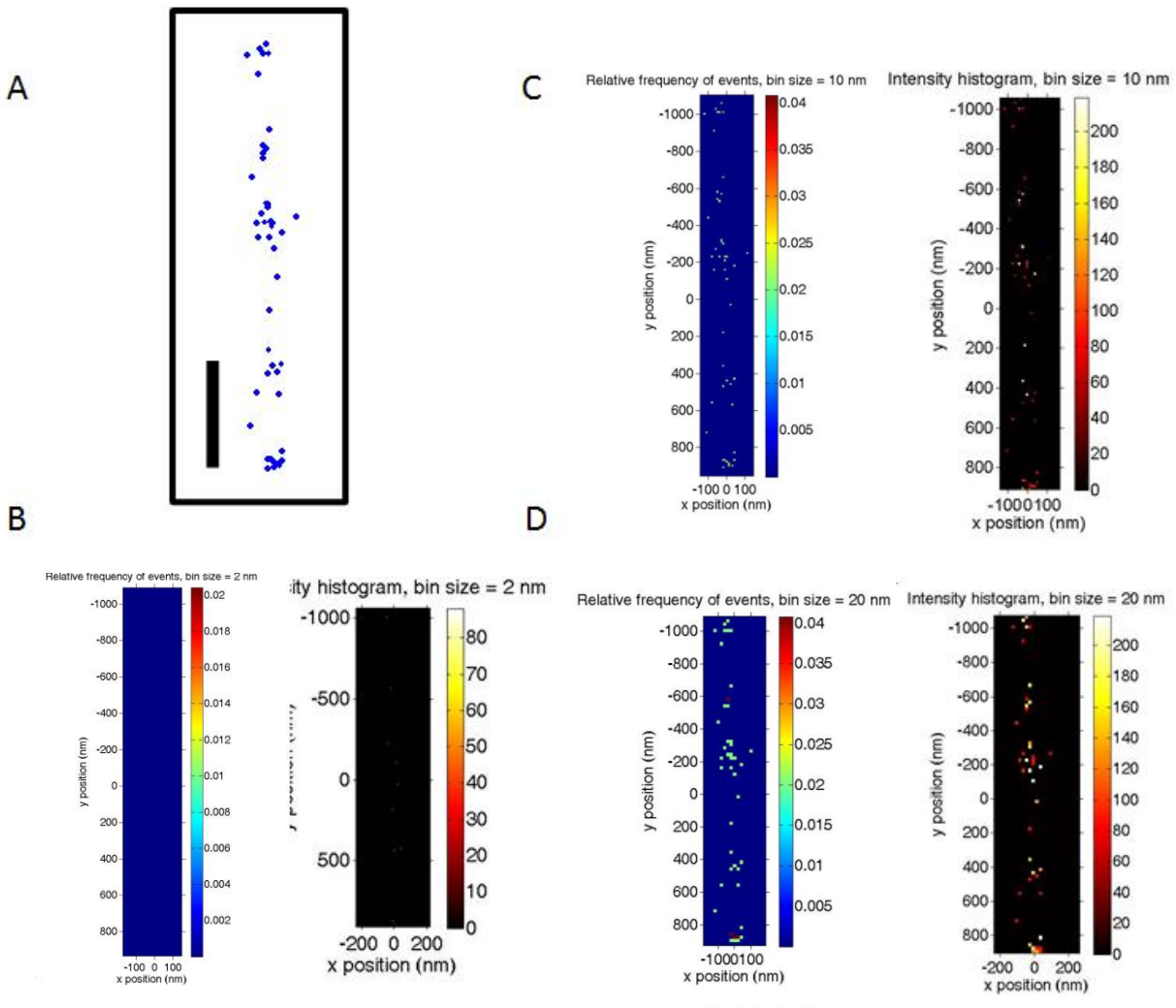

Figure S-18. Data associated with Figure 6 from the manuscript. (A) Scatter plot of centroid points. Scale bar is 500 nm. (B-D) (left) Relative frequency histograms and (right) spatial intensity maps with bin sizes of (B) 2 nm, (C) 10 nm and (D) 20 nm. Scale is as marked.

References:

1 S. Link and M. A. El-Sayed, *Int. Rev. Phys. Chem.*, 2000, **19**, 409.
2 M. B. Mohamed, V. Volkov, S. Link and M. A. El-Sayed, *Chem. Phys. Lett.*, 2000, **317**, 517.
3 H. Kim, C. Xiang, A. G. Guell, R. M. Penner and E. O. Potma, *J. Phys. Chem. C*, 2008, **112**, 12721.
4 H. Lin, S. P. Centeno, L. Su, B. Kenens, S. Rocha, M. Sliwa, J. Hofkens and H. Uji-i, *ChemPhysChem*, 2012, **13**, 973.
5 S. M. Stranahan and K. A. Willets, *Nano Lett.*, 2010, **10**, 3777.